Biomedical Signal Processing and Control 86 (2023) 105056

Contents lists available at ScienceDirect

Biomedical Signal Processing and Control

journal homepage: www.elsevier.com/locate/bspc

QT interval time lag in response to heart rate changes during stress test for Coronary Artery Disease diagnosis

Cristina Pérez [a,*], Esther Pueyo [a,b], Juan Pablo Martínez [a,b], Jari Viik [c], Pablo Laguna [a,b]

[a] Biomedical Signal Interpretation and Computational Simulation (BSICoS) group, Aragón institute of Engineering Research (I3A), IIS Aragón, University of Zaragoza, 50018, Zaragoza, Spain

[b] Biomedical Research Networking Center in Bioengineering, Biomaterials and Nanomedicine(CIBER-BBN), Spain

[c] Faculty of Medicine and Health Technology, Tampere University, 33720, Tampere, Finland

ARTICLE INFO

Keywords:
Sudden Cardiac Death
Coronary Artery Disease
Periodic component analysis
Electrocardiogram
QT-RR relationship
Stress test

ABSTRACT

Background : Slow adaptation of the QT interval to abrupt changes in heart rate (HR) can enhance ventricular heterogeneity and has been suggested as a marker of arrhythmic risk. Most investigations on QT rate adaptation lag have been performed in response to step-like HR changes. However, abrupt HR changes are difficult to induce or observe in ECG recordings under ambulatory conditions.

Objective: We aim to evaluate the power of indices related to the QT lag in response to ramp-like HR changes in stress test to assess CAD risk.

Methods: We quantified the lag between the actual QT series and the memoryless expected QT series, which was obtained by fitting a hyperbolic regression model to the instantaneous QT and HR measurements in stages where their behavior could be assumed stationary. The proposed methodology was applied to analyze ECG stress tests of a subset of 448 patients presenting different risk levels for Coronary Artery Disease (CAD). The QT lag was estimated separately in the exercise and recovery phases.

Results: An increase in the estimated QT lag during exercise (from 25 to 36 s) and a decrease during recovery (from 57 to 39 s) were associated with higher CAD risk. The difference between these lags showed significant capacity for CAD risk stratification.

Conclusion: The QT lag in response to HR changes can be quantified from a stress test. QT lag values in response to ramp-like HR changes are in ranges comparable to those quantified from abrupt HR changes and show clinical significance to stratify CAD risk.

1. Introduction

Coronary artery disease (CAD) is the first cause of death worldwide and often leads to Sudden Cardiac Death (SCD) [1]. Elevated repolarization heterogeneity in the ventricular myocardium can promote ventricular fibrillation resulting in SCD [2]. This dispersion can be exacerbated as different ventricular cells present distinct patterns of repolarization adaptation in response to heart rate (HR) changes.

In recent years, large research efforts have been focused on developing noninvasive strategies based on ECG features to define biomarkers to assess the ventricular repolarization dispersion [3]. For example, the T-wave, reflecting ventricular repolarization in the ECG, and the QT interval, measuring the overall duration of ventricular depolarization and repolarization, have been widely investigated to analyze the risk of severe arrhythmias on top of other purposes like identification of exercise-induced myocardial ischemia [4–6]. The first-ECG-derived-biomarkers objective is to stratify patients for arrhythmic risk, preventing arrhythmias generated from ventricular repolarization alterations. [7,8].

One ECG derived marker that reflects spatio-temporal ventricular repolarization dispersion and has shown capacity for SCD risk identification is the time lag of QT interval accommodation to HR changes (QT/RR hysteresis). Previous studies have highlighted the importance of determining normal and abnormal ranges of QT adaptation dynamics in response to sudden changes in HR as a possible way to characterize the risk for cardiac arrhythmias and SCD [9]. In particular, an increase in the QT rate adaptation time in survivors of acute myocardial infarction has been related to higher likelihood of dying from an arrhythmic cause [10,11]. Other studies have measured the rate adaptation of the QT interval after sudden HR changes due to conversion of atrial fibrillation and have postulated that delayed QT adaptation

* Corresponding author.
E-mail address: cperez@unizar.es (C. Pérez).

https://doi.org/10.1016/j.bspc.2023.105056
Received 11 January 2023; Received in revised form 19 April 2023; Accepted 23 May 2023
Available online 11 June 2023

Table 1
Demographic information in patient groups including HR and QT median values (± interquartile range), in windows W_j, $j \in \{1,2,3\}$, HR_{W_j} and QT_{W_j}, respectively.

	ECG-LR	COR-LR	COR-MR	COR-HR	*p*-value
Clinical variables					
Gender [M/F]	130/83	33/26	16/8	121/31	<0.001
Age (years)	49.0 ± 20.0	52.0 ± 12.8	57.0 ± 15.5	62.0 ± 14.0	<0.001
BMI	25.5 ± 5.5	25.9 ± 6.9	27.1 ± 6.8	26.8 ± 4.8	<0.001
ECG derived variables					
HR_{W_1} (bpm)	80.3 ± 19.7	73.8 ± 16.5	73.6 ± 14.4	65.0 ± 15.2	<0.001
HR_{W_2} (bpm)	167.1 ± 20.2	155.1 ± 31.1	140.0 ± 28.1	116.2 ± 26.3	<0.001
HR_{W_3} (bpm)	98.5 ± 19.7	91.8 ± 21.8	86.9 ± 19.3	73.2 ± 15.0	<0.001
QT_{W_1} (ms)	364.1 ± 37.8	380.0 ± 42.0	377.2 ± 32.9	394.2 ± 40.6	<0.001
QT_{W_2} (ms)	249.6 ± 24.1	268.5 ± 45.8	285.6 ± 32.6	311.4 ± 38.9	<0.001
QT_{W_3} (ms)	343.4 ± 44.8	361.4 ± 49.3	366.7 ± 44.1	387.0 ± 32.1	<0.001

Results are statistically significant ($p < 0.05$) between pairs of groups: *Gender*: COR-HR with ECG-LR and COR-LR; BMI: ECG-LR with COR-HR; *Age*, HR_{W_1}, HR_{W_3}, QT_{W_1}, QT_{W_2} and QT_{W_3}: ECG-LR with COR-LR, COR-MR and COR-HR, COR-LR with COR-HR, and COR-MR with COR-HR. HR_{W_2}: all pairs of groups are statistically significant.

could be a potential risk factor for proarrhythmia [12,13]. To shed light on the cell and tissue mechanisms underlying QT/RR hysteresis and the relationship with arrhythmic risk, experimental, clinical and simulated electrophysiological methods have been used and potential underpinnings have been described [8,14–17].

The QT interval adaptation to sudden changes in HR was evaluated in [10,18,19], and found to follow an exponential-like pattern, implying an underlying first-order system component between RR and QT [20]. This phenomenon occurs on top of beat-to-beat QT interval variability, which is commonly quantified under stationary conditions and can thus provide complementary information [21]. However, the presence and availability of abrupt HR changes (or step-like HR) in Holter recording is not always guaranteed and its distribution can be very variable from subject to subject.

Alternatively, HR changes are observed during an exercise stress test, where the adaptation time of the QT interval to HR changes can be estimated. The easily induced HR changes and the wide range of that reflected during the test offers the opportunity to assess the dynamics of the QT interval in response to changes in HR [5,22]. These HR changes follow a trend comparable to a ramp. Theoretically, the ramp-response of a first-order system is characterized by another ramp delayed by a lag of the same value as the time constant of the step-response [23]. Thus, the use of this test for QT lag estimation is suggested in our work.

Considering that the relationship between the RR and QT time series can be modeled by a first-order system followed by a non-linear relation [20], we suggest expressing the relationship by these two separate blocks and focus on the linear block to characterize the QT lag. We propose a methodology to compute the lag during a stress test as the delay between actual QT and a series of QT values instantaneously estimated (i.e., without memory) from the RR series. This estimated lag should provide clinical information equivalent to that provided by the time constant of the QT response to a step-like HR change. Preliminary results from an exploratory analysis were presented in [24], where the QT lag was automatically derived from ECG signals recording during an exercise stress test.

This procedure requires to measure the QT from exercise stress test ECGs, where the influence of noise, artifacts and even the eventual overlapping of T-wave and P-wave at very high HR complicate the delineation of the T-wave end. Recent studies investigating stress test ECGs incorporate manual delineation to compute the T-wave end, thus implying that the number of patients is necessarily reduced [25], or they simply do not study the dynamics of the QT interval at high HR [26,27]. Therefore, we study and propose different automated procedures in this work to improve the QT delineation in this changing scenario.

The work here presented has three main objectives, all related to the estimation of the QT lag during an exercise stress tests: (1) to assess different lead-space reduction (LSR) techniques for robust computation of the T-wave end in stress test recordings -Section 2-; (2) to develop a method to compute the QT lag during a stress test and propose three different markers related to such QT lag in response to a ramp-like HR change -Section 2-; and (3) to evaluate the power of the proposed markers to assess CAD risk -Section 3-. The QT lags quantified in our study were compared with previous studies that evaluated the QT response to a step-like HR change to verify if they took values in a similar range -Section 4-.

2. Methods

2.1. Database

A total of 528 ECG signals recorded from patients undergoing stress test ECG at Tampere University Hospital (Finland), aimed to characterize patients at high risk of cardiovascular morbidity and mortality [28], were analyzed. A continuous ECG was recorded at a sampling frequency of F_s = 500 Hz with CardioSoft exercise ECG system (Version 4.14, GE Healthcare, Freiburg, Germany), with the Mason-Likar modified 12-lead system. The stress test was performed in a bicycle ergometer. The initial workload varied from 20 W to 30 W, with the load being increased stepwise by a fixed, patient-specific quantity in the range 10–30 W every minute (for females 10–20 W) based on physicians evaluation of patient's condition. This patient-specific quantity is not annotated at the database. Workload was removed immediately after the exercise peak. A total of 80 patients were discarded due to the presence of large artifacts, early finished test or frequent ectopic beats, which did not allow to calculate the QT interval series along the stress test.

Patients were classified into four groups according to their likelihood for CAD. The ECG-LR (LR refers to Low Risk) group was based solely on information from clinical history and the ECG (those patients did not undergo angiography). The remaining patients were classified according to the results of the coronary angiography (COR) depending on whether they presented less than 50% (COR-LR), between 50 and 75% (COR-MR), or more than 75% (COR-HR) of luminal narrowing of the diameter of at least one major epicardial coronary artery or main branches. LR, MR, and HR referring to Low, Mild and High Risk, respectively. All the coronary angiographies were analyzed by the same cardiologist. So, there were 213, 59, 24 and 152 subjects in ECG-LR, COR-LR, COR-MR and COR-HR groups, respectively. Demographic variables and the main information relating to ECG parameters of each group are shown in Table 1.

2.2. Signal preprocessing

The ECG was subject to filtering prior to delineation of its wave boundaries. First, high-frequency noise and artifacts were attenuated by using a 6th-order Butterworth low-pass filter, with cut-off frequency of 50 Hz, implemented in a forward–backward version to avoid ECG distortion by guaranteeing linear phase. Afterwards, baseline wander was attenuated using cubic spline interpolation, for which the isoelectric level at each beat was estimated as the averaged value of the filtered ECG in a 20-ms window starting 80 ms before the QRS fiducial point taken as the R point of the QRS complex.

2.3. Enhancement of T-wave end delineation by spatial signal transformation

Two ECG lead-space reduction (LSR) techniques were applied to the 8 independent standard leads: Principal Component Analysis (PCA) [29] and Periodic Component Analysis (πCA) [30]. These allowed to generate new transformed leads that improve signal-to-noise ratio

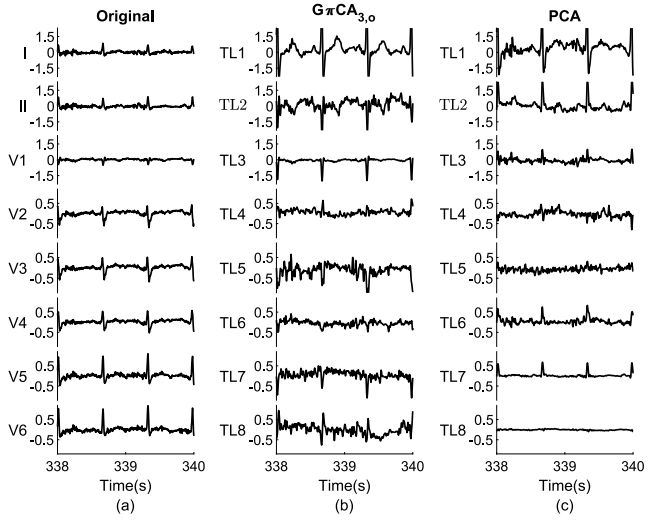

Fig. 1. (a) Example of ECG from 8 independent standard leads recorded during a stress test in mV, (b) their corresponding 8 transformed leads, in mV, obtained with $G\pi CA_{3,o}$ and (c) obtained with PCA, where the emphasized T-waves at TL1 can be appreciated.

(SNR), where delineating waves and extracting features were more accurate, like the QT interval, eventually subject to further processing. This is particularly relevant in the usually very noisy stress test ECG signals. The spatial lead transformation was computed by applying a transformation matrix $\mathbf{\Psi}^T$ to the original leads:

$$\mathbf{y}(n) = \mathbf{\Psi}^T \mathbf{x}(n). \tag{1}$$

where $\mathbf{x}(n)$ is the data vector containing the values of the signals in the L leads, at sample n, columnwise:

$$\mathbf{x}(n) = \begin{bmatrix} x_1(n) & x_2(n) & \dots & x_L(n) \end{bmatrix}^T,$$

and $\mathbf{y}(n)$ contains the corresponding transformed leads:

$$\mathbf{y}(n) = \begin{bmatrix} y_1(n) & y_2(n) & \dots & y_L(n) \end{bmatrix}^T.$$

To calculate the transformation matrix, $\mathbf{\Psi}$, a time window learning period was selected, whose data were piled in matrix $\mathbb{X}_q$, which contains signal excerpts corresponding to T-waves from K beats in the selected window. The T-wave excerpt for each kth beat was taken from sample $n_{\mathrm{QRS}}(k) + (25 + 1.2\mathrm{RR}_m^{1/2})F_s/1000$ to $n_{\mathrm{QRS}}(k) + (300 + 1.2\mathrm{RR}_m^{1/2})F_s/1000$, where $n_{\mathrm{QRS}}(k)$ is the QRS complex fiducial point [31], and RR_m is the median RR interval value (in milliseconds) in the learning window. Each kth beat, lth lead T-wave has a length of N samples and is expressed in vector notation as:

$$\mathbf{x}_{k,l} = \begin{bmatrix} x_{k,l}(1) & x_{k,l}(2) & \cdots & x_{k,l}(N) \end{bmatrix}^T. \tag{2}$$

The T-waves from all L leads of the kth beat were put together into matrix $\mathbf{X}_k$:

$$\mathbf{X}_k = \begin{bmatrix} \mathbf{x}_{k,1} & \mathbf{x}_{k,2} & \cdots & \mathbf{x}_{k,L} \end{bmatrix}^T, \tag{3}$$

where each column contains the nth samples from the kth beat T-waves in all the L leads.

Finally, the matrix $\mathbb{X}_q$ was constructed by concatenating the $\mathbf{X}_k$ matrix from all K beats:

$$\mathbb{X}_q = \begin{bmatrix} \mathbf{X}_1 & \mathbf{X}_2 & \cdots & \mathbf{X}_K \end{bmatrix} \tag{4}$$

Two spatial reduction strategies were considered:

- *Principal Component Analysis* (PCA): this method yields transformed leads guided by a maximum-variance concentration criterion [29]. The orthogonal transformation matrix, now $\mathbf{\Psi} \equiv \mathbf{\Psi}_{\mathrm{PCA}}$, is the eigenvector decomposition matrix of the 8×8 inter-lead ECG autocorrelation matrix $\mathbf{R}_{\mathbb{X}_q}$,

$$\mathbf{R}_{\mathbb{X}_q} \mathbf{\Psi}_{\mathrm{PCA}} = \mathbf{\Psi}_{\mathrm{PCA}} \mathbf{\Lambda}, \tag{5}$$

with $\mathbf{R}_{\mathbb{X}_q}$ estimated from the learning data matrix as

$$\hat{\mathbf{R}}_{\mathbb{X}_q} = \frac{1}{KN} \mathbb{X}_q \mathbb{X}_q{}^T, \tag{6}$$

and $\mathbf{\Lambda}$ being a diagonal matrix containing the eigenvalues of $\mathbf{R}_{\mathbb{X}_q}$ sorted in descending order. $\mathbf{\Psi}_{\mathrm{PCA}}$ contains column-wise the corresponding eigenvectors.

- *Periodic Component Analysis* (πCA): A spatial transformation based on periodic component analysis [32] can be used to maximize a given periodicity in the transformed lead. In [30], this πCA transformation was proposed to emphasize beat-to-beat periodicity in the transformed lead, making use of the beat-to-beat coherence observed in the ECG signal. In highly noisy recordings with low SNR, as stress test ECG, the first transformed lead of PCA can contain noise when this is dominant or comparable in energy (variance) to the true (noiseless) ECG signal. In this study, we hypothesized that the periodicity maximization criterion used by πCA will filter out noise, even in cases of low SNR, provided that it does not have the beat periodicity of the signal. The transformation matrix, now $\mathbf{\Psi} \equiv \mathbf{\Psi}_{\pi\mathrm{CA}}$, is derived as the generalized eigenvector matrix of a matrix pair, ordered in ascending order of eigenvalue magnitude [30]. The πCA transformation can be further generalized, $G\pi CA$ $\mathbf{\Psi} \equiv \mathbf{\Psi}_{G\pi\mathrm{CA}}$, if it is considered that ECG signals are p-beat periodic [13] with p taking values from 1 up to P, $G\pi CA_P$. Then, the generalized eigenvector problem,

$$\mathbf{R}^P_{\Delta\mathbb{X}_{p,q}} \mathbf{\Psi}_{G\pi\mathrm{CA}} = \mathbf{R}_{\mathbb{X}_q} \mathbf{\Psi}_{G\pi\mathrm{CA}} \mathbf{\Lambda}, \tag{7}$$

including the matrix pair $\left(\mathbf{R}^P_{\Delta\mathbb{X}_{p,q}}, \mathbf{R}_{\mathbb{X}_q}\right)$ [13], is solved. The spatial correlation of the non-periodic residual, $\mathbf{R}^P_{\Delta\mathbb{X}}$, is estimated as:

$$R^P_{\Delta\mathbb{X}_{p,q}} = \frac{1}{PKN} \sum_{p=1}^{P} \Delta\mathbb{X}_{p,q} \Delta\mathbb{X}^T_{p,q}, \tag{8}$$

with

$$\Delta\mathbb{X}_{p,q} = \mathbb{X}_{p,q} - \mathbb{X}_q. \tag{9}$$

The matrix $\mathbb{X}_{p,q}$ is $\mathbb{X}_q$ shifted p beats forward. When $G\pi CA_P$ is applied with $P = 1$ (minimizing the non- beat-to-beat periodic component), it results in the regular πCA, $G\pi CA_1 \equiv \pi$CA [30].

The selection of the signal excerpt where to learn the transformation matrix can be relevant for the study. The eigenvector accounts for a kind of smoothed version of the different T-wave morphologies contained in the learning window, aiming to generate a transformed lead better suited for T-wave delineation. Nevertheless, the large dynamics of the HR in stress test could generate doubts about the stability and suitability of this smoothed eigenvector as the best suited when derived from the whole recordings. For this reason, we propose to explore two strategies: unique learning of the transformation matrix on a selected learning window, or a relearning of the transformation matrix every 150 s. The latter was introduced to better account for the long-term T-wave changes (not beat-to-beat), which are the ones relevant to estimate the QT lag from the trend series differences. Depending on the selected strategy for learning the matrix $\mathbf{\Psi}$, six variants of the two LSR techniques were proposed.

- **πCA**: or $G\pi CA_1$, where the transformation was learnt in each signal window of 150 s, recalculating the $\mathbf{\Psi}$ matrix in each window, for $P = 1$.

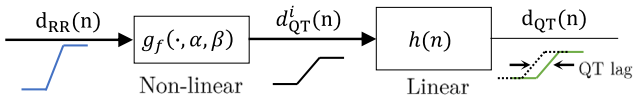

Fig. 2. Schematic diagram of the relationship between the RR and QT interval series during a stress test. First, a non-linear transformation $g(\cdot,\alpha,\beta)$ is applied to the RR series to obtain an instantaneous memoryless QT series $d^i_{QT}(n)$. This is followed by a first-order linear system (impulse response $h(n)$) generating the QT series $d_{QT}(n)$, which allows computing the QT memory as the lag between the QT series $d^i_{QT}(n)$ and $d_{QT}(n)$ QT series.

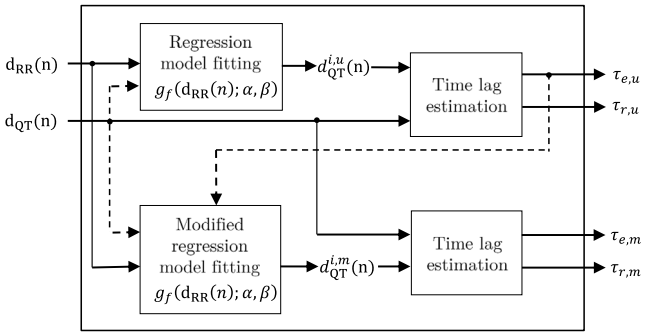

Fig. 3. Diagram for the QT time lag computation process, in the exercise and recovery phases of a stress test using either unmodified or modified instantaneous QT series estimation ($d^{i,u}_{QT}(n)$ and $d^{i,m}_{QT}(n)$ respectively). Broken lines denote accessory input information required for estimation of the parameters α and β.

- Gπ**CA**$_3$: where the transformation was learnt in each window of 150 s with recalculation of the Ψ matrix, with $P = 3$.
- π**CA**$_o$: GπCA$_{1,o}$, where the Ψ matrix was estimated once using the first 150 s at the onset of the signal, and then the same transformation Ψ was applied to the rest of signal, with $P = 1$.
- Gπ**CA**$_{3,o}$: The Ψ matrix was estimated once using information at signal onset, in the first 150 s, and then applied to the complete signal, with $P = 3$.
- **PCA**: PCA technique where Ψ matrix was reestimated in each window of 150 s.
- **PCA**$_o$: PCA technique where Ψ matrix was estimated once at the signal onset, using the information of the first 150 s, and then applied to the complete signal.

An example of the 8 standard leads of an ECG recording and the transformed leads of both LSR techniques are shown in Fig. 1. It can be observed how the T-wave in the first transformed lead, in TL1, of both GπCA$_3$ and PCA, is emphasized, being more remarkable for GπCA$_3$. T-wave delineation is then performed.

2.4. QT memory lag estimation methodology

After studying the best LSR technique to delineate the T-wave end point, $n_{Te}(k)$, the computation of the RR and QT series was calculated. The process to estimate the time lag of the QT interval series following the RR interval series could be divided in two main steps: the calculation of an expected instantaneous memoryless, HR-dependent QT interval series (corresponding to the non-linear QT to RR dependency), and the QT time lag estimation between the real QT, and the instantaneous memoryless HR-dependent QT interval series (related by a linear system). The process is summarized in the diagram of Fig. 2. Moreover, a more detailed diagram about the calculation of the different lags was represented in Fig. 3.

2.4.1. RR and QT series estimation

The single-lead wavelet-based algorithm [33] was used to extract both the RR, $d_{RR}(k)$, and the QT, $d_{QT}(k)$, intervals series from each lead. After single-lead delineation, a multi-lead (*MLeads*) strategy was applied to the delineation marks of the 8 independent standard leads to assign a unique mark to a beat. Using those unique marks, the time series $d_{RR}(k) = n_{QRS}(k) - n_{QRS}(k-1)$ was calculated and the QRS onset point, $n_{QRSo}(k)$, was estimated. The T-wave end points, $n_{Te}(k)$, were extracted either from the multi-lead delineation strategy or alternatively by computing a single-lead delineation in the first transformed lead $y_1(n)$ (TL1) for each of the six variants of the LSR techniques described before, from which the time series $d_{QT}(k) = n_{Te}(k) - n_{QRSo}(k)$ was calculated.

Outlier values of both $d_{RR}(k)$ and $d_{QT}(k)$ series, identified as those deviating by more than $\pm 10\%$ or $\pm 5\%$, respectively, from the running median of each series computed over 40 consecutive beats were replaced with the corresponding median value. Subsequently, missing points were interpolated using a piecewise cubic Hermite polynomial. In most cases, these missed points were near stress peak and there was not a long time interval without any QT measure. Using piecewise cubic Hermite polynomial avoids overshoots and a larger oscillation if the data are not smooth. This process helped to emphasize the series trends and facilitate the estimation of the QT memory lag, which was based on a mean square error criterion. Finally, $d_{RR}(k)$ and $d_{QT}(k)$ series were interpolated to 4 Hz to have uniformly sampled $d_{RR}(n)$ and $d_{QT}(n)$ time series. Examples can be observed in Fig. 5a.

To compare the performance of the six different LSR transformation techniques presented in Section 2.3, the variability of the raw unfiltered interpolated QT interval series, without removing outlier values, $d^r_{QT}(n)$, was estimated as the power of the 0.04 Hz cut-off high-pass filtered interval series, separately in exercise and recovery phases. Under the assumption that delineation errors are uncorrelated to the (method-invariant) physiological variability of the QT interval, the power of the filtered series ($\mathcal{P}_{QTV}$) includes both the natural variability of QT interval (common for the seven methods) and the power of the delineation errors. Therefore, $\mathcal{P}_{QTV}$ was considered as a surrogate for delineation performance: the lower $\mathcal{P}_{QTV}$, the better performance. Some interpolated QT interval series, before and after removing outlier values, $d^r_{QT}(n)$ and $d_{QT}(n)$ respectively, are shown in Fig. 4, where T-wave delineation was performed in a transformed lead in some examples. The automatic process to compute the onset of the exercise ramp and the end of the recovery ramp is described in Section 2.4.3.

2.4.2. Expected instantaneous memoryless HR-dependent QT

Before calculating the time lag of the $d_{QT}(n)$ series following the $d_{RR}(n)$ series during the assumed linear HR trends in the stress and recovery phases, we realized that an intermediate series had to be computed. This new series kept the temporal variation of $d_{RR}(n)$, but their values were comparable to $d_{QT}(n)$ series. This is a consequence of the non-linear relationship between the RR and QT time series, in addition to a delay well modeled by a first order system [20]. We separated these two blocks, see Fig. 2, and restricted the analysis to the linear part, which characterizes the QT memory lag. Specifically, we first considered a non-linear block component that relates the RR with the corresponding QT if conditions were stationary, generating the so called expected instantaneous memoryless, HR-dependent QT interval denoted as $d^i_{QT}(n)$. This was followed by the linear block that just introduced the memory connecting $d^i_{QT}(n)$ with the actual QT value $d_{QT}(n)$. Then, the lag was obtained as an estimate of the delay between the ramps of these two series when the input was of the ramp-like type. This modeling is the same already presented in [20], but with a shift in the order of the linear and nonlinear blocks. The $d^i_{QT}(n)$ series contains the QT values that would correspond to each $d_{RR}(n)$ value if the HR was stationary in previous beats. To compute $d^i_{QT}(n)$, the following

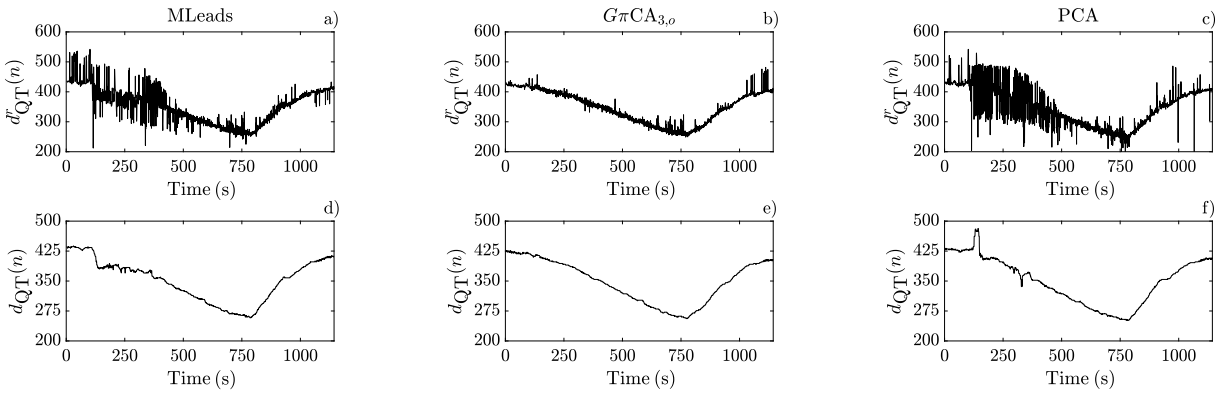

Fig. 4. Examples of $d_{QT}(n)$ series using, (a) and (d), the multi-lead strategy with the 8 independent standard leads, (b) and (e), the first $G\pi CA_{3,o}$ transformed lead, and (c) and (f) the first PCA transformed lead to compute the T_e points. The first row correspond to the $d'_{QT}(n)$ series and the second row to the $d_{QT}(n)$ including the running median filter for outlier rejection.

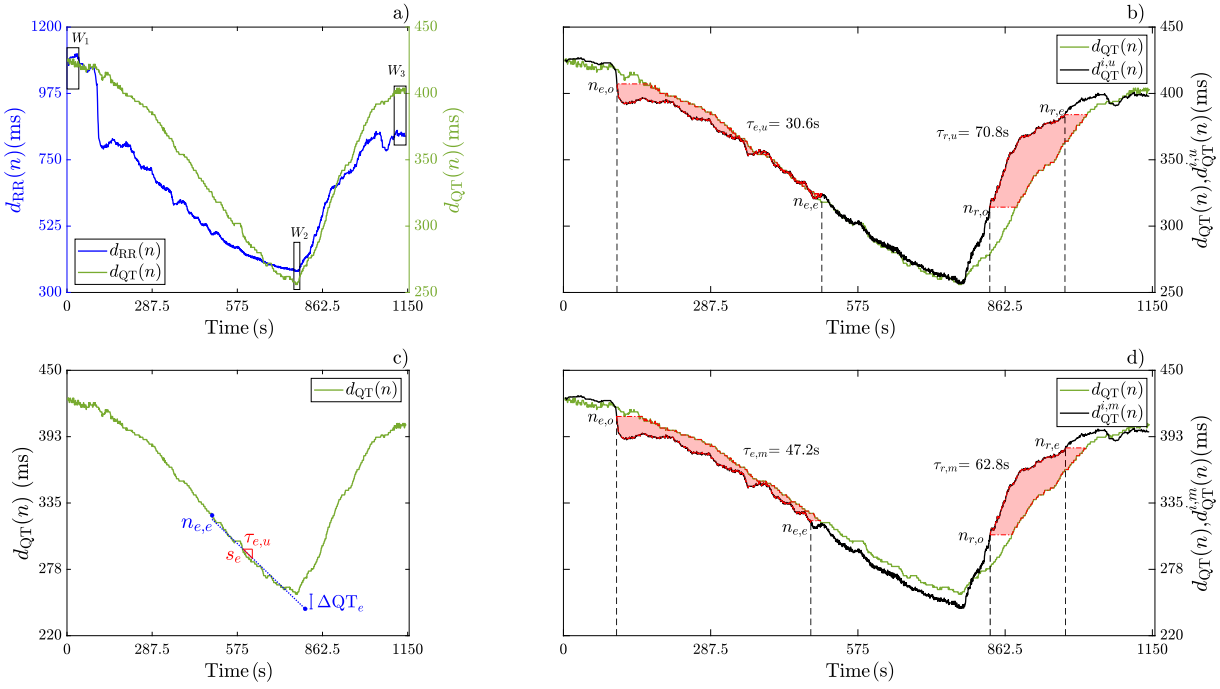

Fig. 5. Example of the procedure for time lag estimation in an ECG-LR subject. (a) Overploted boxes over $d_{RR}(n)$ series defining the three windows, W_1, W_2, and W_3, used to estimate α and β parameters. (b) Ramp delimitation onset, and end, sample points in exercise ($n_{e,o}$, $n_{e,e}$) and recovery ($n_{r,o}$, $n_{r,e}$), with their corresponding lags obtained by minimizing the MSE criteria between $d_{QT}(n)$ and $d^{i,u}_{QT}(n-\tau)$. (c) Graphical representation of the procedure to obtain the ΔQT value to modify $d_{QT}(n)$ at the W_2 window in stress peak using $\tau_{e,u}$ derived as in (b). (d) The corresponding exercise and recovery time lags obtained after regression estimation from the modification of the QT values in (c).

expression was used, where g_f is one of the regression models shown in Table 2:

$$\tilde{d}^{i}_{QT}(n) = g_f(\tilde{d}_{RR}(n); \alpha, \beta), \tag{10}$$

where the tilde over $\tilde{d}_X(n)$, $X \in \{QT, RR\}$, indicates that the series are expressed in seconds, $\tilde{d}_X(n) = d_X(n)/1000$, rather than milliseconds. The values of the parameters α and β for the g_f regression models of Table 2 were obtained by fitting $[\tilde{d}_{QT}(n), \tilde{d}_{RR}(n)]$ data pairs, from three windows simultaneously: W_1 taken before the stress onset (40 s), W_2 taken at the stress peak (20 s) and W_3 taken before the test end (40 s). The values of $d_{QT}(n)$ and $d_{RR}(n)$ were assumed to be stationary in these windows and representative of the subject instantaneous QT-to-RR dependency. These window areas are marked with boxes in Fig. 5(a). The four regression models considered in the study were parabolic ($f \equiv$ Par), linear ($f \equiv$ Lin), hyperbolic ($f \equiv$ Hyp) and logarithmic ($f \equiv$ Log). Model parameters were estimated using weighted least squares with the data in W_1, W_2 and W_3, where W_2 was replicated twice to have the three regions equally weighted in the estimation.

The assumption of stationarity at the stress peak, W_2, is questionable, but it was included to account for the whole excursion of RR when evaluating the QT-to-RR dependency. To mitigate this drawback, two different strategies to estimate the regression parameter values, $\hat{\alpha}$ and $\hat{\beta}$, were considered. As one strategy depends on an initial QT lag calculated with the other strategy, a block diagram that summarizes this computation is shown in Fig. 3.

QT-to-RR regression estimation from the unmodified QT series. In this approach, corresponding to the top block of Fig. 3, the window W_2 was taken to be symmetric around the minimum value of $d_{RR}(n)$ at the stress peak, thus including QT values from HR acceleration and deceleration phases, with opposite effects on the QT interval. We hypothesized that this definition of W_2 will compensate for the QT dynamics under HR acceleration and deceleration and it will make the mean QT-to-RR relationship not far from that under stationary conditions.

From the three windows W_1, W_2 and W_3, a least-squares fit of the unmodified (actual) $[\tilde{d}_{QT}(n), \tilde{d}_{RR}(n)]$ data pairs was performed for each

tested regression model and patient-specific values of $\hat{\alpha} \equiv \hat{\alpha}_u$ and $\hat{\beta} \equiv \hat{\beta}_u$ were obtained, where the subscript "u" stands for use of *unmodified* data in their estimation. The corresponding expected instantaneous, memoryless, HR-dependent QT interval series, $d^{i,u}_{\mathrm{QT}}(n)$, was calculated all along the stress test (exercise and recovery) by applying the regression formula in (10) for each of the regression models in Table 2, making use of the $\hat{\alpha}_u$ and $\hat{\beta}_u$.

QT-to-RR regression estimation from the modified QT series. The second approach, corresponding to the bottom block of Fig. 3, tried to account for the fact that the RR and QT series being at comparable stationary states may not hold at the stress test peak, i.e. window W_2, since QT requires some seconds after the HR trend changes to converge to a new stationary state. Therefore, we propose to modify the actual QT values at peak window W_2 by a fixed amount, which accounts for the delay we know the trend of QT series has in following RR trend changes. So the resulting [QT, RR] pairs, after QT modification, will be a better comparable stationary QT-to-RR dynamic in window W_2. An initial QT lag value calculated at the exercise, "e", phase from the QT series estimated in the unmodified, "u", approach described in Section 2.4.2, $\tau_{e,u}$, was computed using the method presented in Section 2.4.3. This $\tau_{e,u}$ was used to modify the $d_{\mathrm{QT}}(n)$ values at window W_2, generating a *modified* series $d_{\mathrm{QT}_m}(n) = d_{\mathrm{QT}}(n) - \Delta\mathrm{QT}$, denoted by subscript "$m$". The subtracting factor ΔQT results from multiplying $\tau_{e,u}$ by the absolute value of the QT series slope at the stress peak, s_e ($\Delta\mathrm{QT} = \tau_{e,u} \times s_e$).

The s_e value was calculated as the absolute value of the slope of the linear fit to the QT series from the selected end of the exercise ramp, $n_{e,e}$, defined in Section 2.4.3, to the point associated with the lowest $d_{\mathrm{QT}}(n)$ value, see Fig. 5c. In doing so, it was assumed that the QT values that represent the QT-to-RR stationary dependency at W_2 were the real ones, $d_{\mathrm{QT}}(n)$, but decreased by the quantity ΔQT, which is an estimate of the value that would have been attained if the stress phase had lasted for an extra $\tau_{e,u}$ time at the same HR, required to converge to the QT stationary value. Thus, the modified data pairs in W_2 became $[\tilde{d}_{\mathrm{QT}_m}(n), \tilde{d}_{\mathrm{RR}}(n)]$, which were used together with data in W_1 and W_3 to estimate the modified model parameters values $\hat{\alpha} \equiv \hat{\alpha}_m$ and $\hat{\beta} \equiv \hat{\beta}_m$. A graphic example of this process can be seen in Fig. 5c. The resulting time series estimated after applying the same regression formula as in (10) was denoted as $d^{i,m}_{\mathrm{QT}}(n)$.

For both strategies, the root mean square error

$$\varepsilon^{u}_{\mathrm{rms}} = \sqrt{\frac{1}{3\times 40\times 4}\sum_{n\in\{W_j\}}\left(d_{\mathrm{QT}}(n) - d^{i,u}_{\mathrm{QT}}(n)\right)^2}, \tag{11}$$

and

$$\varepsilon^{m}_{\mathrm{rms}} = \sqrt{\frac{1}{3\times 40\times 4}\sum_{n\in\{W_j\}}\left(d_{\mathrm{QT}_m}(n) - d^{i,m}_{\mathrm{QT}}(n)\right)^2}, \tag{12}$$

measuring the goodness of fit of the QT-to-RR relationship in the fitting windows W_j, $j \in \{1, 2, 3\}$. This value was used to evaluate the model fitting. Note that $d_{\mathrm{QT}_m}(n) \equiv d_{\mathrm{QT}}(n)$ in W_1 and W_3.

2.4.3. QT time lag estimation

The time lag between $d^{i}_{\mathrm{QT}}(n)$ and $d_{\mathrm{QT}}(n)$ time series (example in Fig. 5b and d) was estimated as the τ resulting in a minimum Mean Square Error (MSE) difference between the $d_{\mathrm{QT}}(n)$ ramp segment, during stress or recovery, and their corresponding delayed $d^{i}_{\mathrm{QT}}(n-\tau)$ ramp segment. This estimation was performed separately at stress and recovery, and the time lag providing the minimum MSE, τ_e in stress or τ_r in recovery, was estimated by comparing the curves from exercise onset, $n = n_{e,o}$, to exercise end, $n = n_{e,e}$, for τ_e, and from recovery onset, $n = n_{r,o}$, to recovery end, $n = n_{r,e}$, for τ_r, as marked in Fig. 5b. This procedure was followed for both QT unmodified and modified strategies at W_2 for regression parameter estimation, see Fig. 5b and d.

The difference between the adaptation lags in stress and recovery, Δ_τ, was also computed and studied as an additional marker to stratify for CAD risk:

$$\Delta_\tau = \tau_r - \tau_e. \tag{13}$$

An automatic procedure was designed to determine exercise and recovery ramp boundaries (i.e. onsets and ends). The exercise onset, $n_{e,o}$ (analogously the recovery end, $n_{r,e}$), was taken as the point resulting in minimum mean squared differences between $d^{i}_{\mathrm{QT}}(n)$ series and a piecewise linear approximation consisting on a plateau (incline, for $n_{r,e}$) until the candidate point, followed by a subsequent incline (plateau, for $n_{r,e}$). In mathematical terms, the search for $n_{e,o}$ resulted from minimizing the following cost function [34]:

$$n_{e,o} = \arg\min_k(J(k)), \tag{14}$$

where

$$J(k) = \sum_{n=M_1}^{k-1}\left(d^{i}_{\mathrm{QT}}(n) - f_b(n)\right)^2 + \sum_{n=k}^{M_2}\left(d^{i}_{\mathrm{QT}}(n) - f_a(n)\right)^2. \tag{15}$$

The functions $f_b(n) = a_b + b_b n$ and $f_a(n) = a_a + b_a n$ were the best linear models fitted in the least squares sense of $d^{i}_{\mathrm{QT}}(n)$ series before and after the candidate sample point k, respectively, being $M_1 = 1$ and $M_2 = n_p - 800$, with n_p the sample corresponding to stress peak value. Analogously, for $n_{r,e}$ the same minimization was performed, but now $M_1 = n_p + 320$ and M_2 is the last sample in $d^{i}_{\mathrm{QT}}(n)$.

The end of the exercise ramp, $n_{e,e}$, was defined as the first sample for which $d^{i}_{\mathrm{QT}}(n)$ shortened from $n_{e,o}$ by a percentage, $100\gamma_e$% of the total reduction reached at the stress peak:

$$n_{e,e} = \arg\min_n\left|\gamma_e\left(d^{i}_{\mathrm{QT}}(n_{e,o}) - d^{i}_{\mathrm{QT}}(n_p)\right) - \left(d^{i}_{\mathrm{QT}}(n_{e,o}) - d^{i}_{\mathrm{QT}}(n)\right)\right|. \tag{16}$$

In a similar way, the onset of the recovery ramp, $n_{r,o}$, was identified as the first sample for which $d^{i}_{\mathrm{QT}}(n)$ increased by a percentage $100\gamma_r$% of the total increase reached at $n_{r,e}$:

$$n_{r,o} = \arg\min_n\left|(1-\gamma_r)\left(d^{i}_{\mathrm{QT}}(n_{r,e}) - d^{i}_{\mathrm{QT}}(n_p)\right) - \left(d^{i}_{\mathrm{QT}}(n_{r,e}) - d^{i}_{\mathrm{QT}}(n)\right)\right|. \tag{17}$$

The optimum threshold values γ^*_e and γ^*_r were chosen as the ones maximizing the significance of the estimated τ in separating CAD risk groups. $\gamma_e = 1$ and $\gamma_r = 0$ are equivalent to placing $n_{e,e}$ and $n_{r,o}$, respectively, at the stress peak n_p.

To estimate the significance, firstly, the threshold values were varied in the range [0.30, 1.00], for exercise, and in the range [0.00, 0.70], for recovery, in steps of 0.05, to calculate the corresponding delays, Fig. 6a and b. Then, the p-value for the comparison between each pair of groups was calculated along the different thresholds, Fig. 6c, and d. Lastly, the mean p-value, p_m, of the ones obtained for groups pairs who has resulted in significant differences in more than half of the considered thresholds, was calculated in exercise, p^e_m, and recovery p^r_m, respectively, Fig. 6e, and f. The selected thresholds γ^*_e and γ^*_r were the ones corresponding to minimum of p^e_m and p^r_m, for exercise and recovery, respectively.

2.5. Coronary artery disease risk quantification and statistical analysis

The QT lag had been estimated on the CAD patients described in Section 2.1 and analyzed for its value as CAD risk predictor. All data are presented as median value ± interquartile range. In multiple comparisons, Kruskal–Wallis test is used to assess differences in continuous clinical and ECG variables.

Mann–Whitney U test was applied to continuous variable pairwise comparisons, also when assessing the three proposed markers, i.e. τ_e, τ_r and Δ_τ, selecting the best LSR variant in computing $d_{\mathrm{QT}}(n)$ and in the selection of γ_e and γ_r. Chi-square test was applied to assess differences

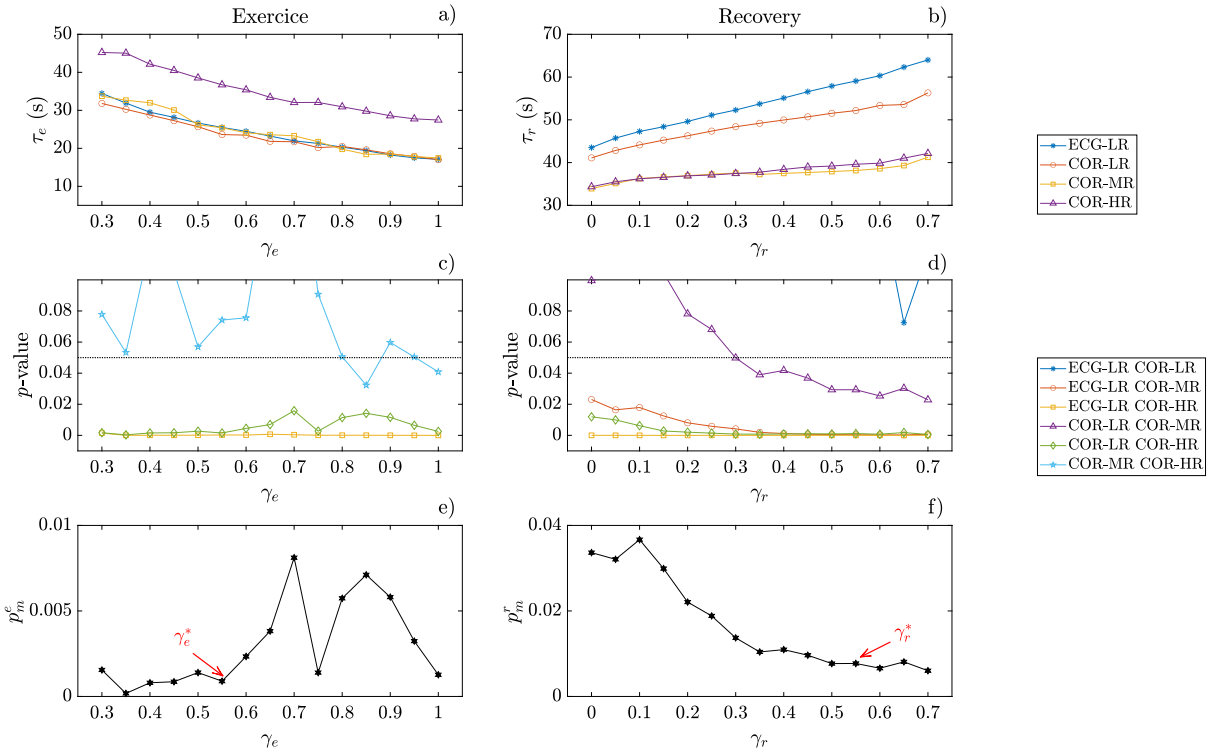

Fig. 6. (a) $\tau_{e,u}$ and (b) $\tau_{r,u}$, values function of the position of $n_{e,e}$, and $n_{r,o}$, obtained by varying thresholds γ_e and γ_r, respectively. (c), and (d), plot the corresponding p-values from (a), (b), respectively, for distinguish between different pairs of patient groups. The broken lines correspond to the significant level, $p = 0.05$. (e) Evolution of p^e_m obtained by varying thresholds γ_e, and (f) p^r_m varying γ_r. For p^e_m and p^r_m calculation the p-values corresponding to group pairs having at least half of the studied thresholds resulting in significant p-values, below dotted lines in panels (c) and (d), are taking into account. Selected thresholds γ^*_e and γ^*_r are marked with red arrows.

in the categorical variable Gender (v_g). $p < 0.05$ was considered statistically significant. The Pearson correlation coefficient was calculated to analyze the relationship between demographic parameters and the proposed QT lag markers. In case of categorical variable gender, a t-test was used to study the group differences between the two gender groups.

Also, a linear mixed model was built for each of the three proposed markers, following the equation:

$$z_{ij} = (\lambda_0 + u_i) + \lambda_1 v_{a_{i,j}} + \lambda_2 v_{b_{i,j}} + \lambda_3 v_{g_{i,j}} + \epsilon_{ij} \tag{18}$$

where z is one of the proposed markers, $z \in \{\tau_e, \tau_r, \Delta_\tau\}$, λ are the fixed-effects regression coefficients, u_i is the random intercept parameter for each of the four risk groups, $v_{a_{i,j}}$ is the age, $v_{b_{i,j}}$ is the BMI, $v_{g_{i,j}}$ is the gender variables, and ϵ represents the residuals. The subscripts i and j refer to ith risk-group and jth patient, respectively.

The Spearman correlation coefficient was computed to study the correlation between each of the proposed QT rate adaptation markers and the degree of stenosis. As the exact degree of stenosis of each patient was unknown and only information on the range of stenosis for each risk group was available, a fixed degree of stenosis was defined for all patients in the same risk group, which corresponded to the mean value of the corresponding range. Thus, patients belonging to COR-LR (stenosis < 50%), COR-MR (stenosis between 50 and 75%), and COR-HR groups (stenosis between 75 and 100%) were assigned with stenosis levels of 25%, 65,5%, and 87.5%, respectively.

3. Results

Demographic information for each patient group together with median HR and QT values in windows W_j, $j \in \{1, 2, 3\}$, HR_{W_j} and QT_{W_j}, respectively, are given in Table 1. Median (and interquartile range) age, BMI and the proportion of males vs females were higher in groups with higher CAD risk. Median HR at stress peak, HR_{W_2}, decreased significantly with increasing CAD risk.

The QT series $d_{QT}(n)$ was calculated by delineating the ECG in the first transformed lead TL1 after applying each of the six different LSR variants of the methodology described in Section 2.3. Fig. 4 presents, in the first row, the unfiltered $d^r_{QT}(n)$ series before applying the median filter. In the second row, the corresponding $d_{QT}(n)$ series after applying the median filter are displayed, evidencing that the presence of outlier values can modify the shape of the $d_{QT}(n)$ series trend. To compare the different methods, the power of the 0.04 Hz high-pass filtered $d^r_{QT}(u)$ series, $\mathcal{P}_{QTV}$, was computed during both exercise and recovery phases for all subjects and results are shown in Fig. 7. Median $\mathcal{P}_{QTV}$ was lower for any LSR technique than when a multi-lead delineation strategy was used to obtain the $n_{Te}(k)$ points. Also, πCA-based methods showed better results than PCA, both in exercise and recovery. Moreover, from Fig. 7 it can be seen that there are no significant differences among πCA-based methods. Therefore, $G\pi CA_{3,o}$ method was selected for the analysis of the clinical data since calculating the transformation matrix once avoids introducing additional abrupt variations in the QT interval series which could occasionally appear due to significant transformation matrix changes when moving along consecutive windows.

The mean and standard deviation of $\hat{\alpha}$ and $\hat{\beta}$ values estimated to generate the expected $d^{i,u}_{QT}(n)$ and $d^{i,m}_{QT}(n)$ series, together with the corresponding ε_{rms}, are shown in Table 2. The lowest ε_{rms} was obtained with the hyperbolic model, so the $d^{i,u}_{QT}(n)$ and $d^{i,m}_{QT}(n)$ were calculated with this model for the remaining part of the 2rbox analysis.

Fig. 6 presents the p-values obtained for patients classification according to CAD risk with time lags obtained for different thresholds γ_e in fixing the exercise end, $n_{e,e}$, and γ_r in fixing recovery onset, $n_{r,o}$, points. To choose optimum γ^*_e and γ^*_r, we analyzed the mean p-value p^e_m and p^r_m evolution. The pairs of groups selected to calculate the mean p^e_m

Table 2
Mean and standard deviation values for the coefficients $\hat{\alpha}$ and $\hat{\beta}$ of different models, and the root mean square error, ϵ_{rms}, in milliseconds. Each fitting was computed using as unmodified QT series, $d^{i,u}_{\text{QT}}(n)$, as modified QT series, $d^{i,m}_{\text{QT}}(n)$.

f	$\tilde{d}^{i}_{\text{QT}}(n) = g_f(\tilde{d}_{\text{RR}}(n);\alpha,\beta)$			ECG-LR	COR-LR	COR-MR	COR-HR
Parabolic log/log (Par)	$\tilde{d}^{i}_{\text{QT}}(n) = \beta(\tilde{d}_{\text{RR}}(n))^{\alpha}$	$d^{i,u}_{\text{QT}}(n)$	$\hat{\alpha}_u$	0.52 ± 0.08	0.49 ± 0.09	0.47 ± 0.08	0.42 ± 0.07
			$\hat{\beta}_u$	0.43 ± 0.03	0.43 ± 0.03	0.43 ± 0.03	0.42 ± 0.02
			$\epsilon^{u}_{\text{rms}}$	8.79 ± 5.27	9.02 ± 6.56	8.74 ± 4.81	7.34 ± 5.66
		$d^{i,m}_{\text{QT}}(n)$	$\hat{\alpha}_m$	0.55 ± 0.09	0.51 ± 0.10	0.49 ± 0.09	0.46 ± 0.08
			$\hat{\beta}_m$	0.44 ± 0.04	0.44 ± 0.04	0.43 ± 0.03	0.42 ± 0.02
			$\epsilon^{m}_{\text{rms}}$	9.67 ± 5.56	9.88 ± 7.09	9.38 ± 5.36	8.12 ± 5.81
Linear (Lin)	$\tilde{d}^{i}_{\text{QT}}(n) = \beta + \alpha\ \tilde{d}_{\text{RR}}(n)$	$d^{i,u}_{\text{QT}}(n)$	$\hat{\alpha}_u$	0.30 ± 0.07	0.27 ± 0.07	0.25 ± 0.07	0.22 ± 0.05
			$\hat{\beta}_u$	0.15 ± 0.03	0.17 ± 0.04	0.18 ± 0.03	0.21 ± 0.03
			$\epsilon^{u}_{\text{rms}}$	10.44 ± 5.88	10.57 ± 7.16	10.00 ± 5.60	8.39 ± 6.19
		$d^{i,m}_{\text{QT}}(n)$	$\hat{\alpha}_m$	0.31 ± 0.07	0.29 ± 0.07	0.26 ± 0.07	0.23 ± 0.05
			$\hat{\beta}_m$	0.14 ± 0.03	0.16 ± 0.04	0.17 ± 0.04	0.19 ± 0.03
			$\epsilon^{m}_{\text{rms}}$	11.25 ± 6.12	11.35 ± 7.58	10.58 ± 6.05	9.16 ± 6.33
Hyperbolic (Hyp)	$\tilde{d}^{i}_{\text{QT}}(n) = \beta + \frac{\alpha}{\tilde{d}_{\text{RR}}(n)}$	$d^{i,u}_{\text{QT}}(n)$	$\hat{\alpha}_u$	−0.08 ± 0.01	−0.09 ± 0.02	−0.09 ± 0.02	−0.10 ± 0.02
			$\hat{\beta}_u$	0.47 ± 0.03	0.49 ± 0.04	0.50 ± 0.04	0.51 ± 0.04
			$\epsilon^{u}_{\text{rms}}$	5.12 ± 3.55	5.87 ± 3.92	5.18 ± 2.48	5.13 ± 4.69
		$d^{i,m}_{\text{QT}}(n)$	$\hat{\alpha}_m$	−0.08 ± 0.01	−0.09 ± 0.02	−0.10 ± 0.02	−0.11 ± 0.03
			$\hat{\beta}_m$	0.48 ± 0.04	0.50 ± 0.04	0.50 ± 0.04	0.52 ± 0.05
			$\epsilon^{m}_{\text{rms}}$	5.49 ± 3.48	6.31 ± 4.13	5.55 ± 2.70	5.63 ± 4.76
Logarithmic (Log)	$\tilde{d}^{i}_{\text{QT}}(n) = \beta + \alpha\ \ln(\tilde{d}_{\text{RR}}(n))$	$d^{i,u}_{\text{QT}}(n)$	$\hat{\alpha}_u$	0.16 ± 0.02	0.16 ± 0.03	0.15 ± 0.03	0.15 ± 0.03
			$\hat{\beta}_u$	0.42 ± 0.02	0.42 ± 0.03	0.42 ± 0.02	0.41 ± 0.02
			$\epsilon^{u}_{\text{rms}}$	6.90 ± 4.33	7.53 ± 5.62	7.40 ± 3.86	6.49 ± 5.23
		$d^{i,m}_{\text{QT}}(n)$	$\hat{\alpha}_m$	0.17 ± 0.03	0.16 ± 0.03	0.16 ± 0.03	0.16 ± 0.03
			$\hat{\beta}_m$	0.42 ± 0.03	0.44 ± 0.03	0.42 ± 0.03	0.42 ± 0.02
			$\epsilon^{m}_{\text{rms}}$	7.53 ± 4.43	8.17 ± 5.93	7.87 ± 4.22	7.13 ± 5.32

were [ECG-LR,COR-HR] and [COR-LR,COR-HR], as these were found to be significantly different for at least half of the analyzed threshold values (see Fig. 6c). In the recovery case, the pairs of groups selected to calculate the mean p-value p^{r}_{m}, were: [ECG-LR,COR-HR], [COR-LR,COR-HR], [ECG-LR,COR-MR] and [COR-LR,COR-MR]. It can be observed from the figure how the closest the ramps delimitation gets to the stress peak (lower γ_r, higher γ_e), the lowest the significance is. γ^{*}_{e} and γ^{*}_{r} were taken where p^{e}_{m} and p^{r}_{m} already converged to a stable minimum plateau, specifically in the extreme of these plateau that provided the largest ramps, that is the largest γ_e and lowest γ_r within the plateau, Fig. 6, so to guarantee reliable τ estimates. After inspection of Fig. 6e and f, values of $\gamma^{*}_{e} = \gamma^{*}_{r} = 0.55$ were selected.

The estimated lags between $d^{i,u}_{\text{QT}}(n)$ and $d_{\text{QT}}(n)$ for each group are shown in Fig. 8. The mean lag $\overline{\tau}_{e,u}$, $\overline{\tau}_{e,u}$, increased with CAD risk (Fig. 8a). Statistically significant differences were only found between low risk groups and COR-HR group. A reverted behavior was observed for mean lag $\overline{\tau}_{r,u}$, as observed from Fig. 8b, where the lag was reduced with CAD risk. In this case, statistically significant differences were found between ECG-LR with COR-MR and COR-HR groups, and between COR-LR with COR-MR and COR-HR groups too.

In view of this asymmetric behavior, the difference in the adaptation time Δ_{τ} was also computed and results are shown in Fig. 8c, $\Delta_{\tau_u} = \tau_{r,u} - \tau_{e,u}$, was larger in ECG-LR and COR-LR patients than in COR-MR ($p = 0.064$, $p = 0.451$, respectively) and COR-HR ($p < 0.001$, $p = 0.002$, respectively) patients.

Moreover, the results of the Pearson correlation coefficient between each proposed QT lag marker and the three demographic variables are presented in Table 3. We can observe a modest linear relationships between the confounding variables and the proposed markers, even if p-values indicate statistical significance. The linear mixed model of the demographic variables reflects a variance of the random parameter of 3.7% (16 of 435), 8.2% (44 of 538) and 9.2% (102 of 1207) for $\tau_{e,u}$, $\tau_{r,u}$ and Δ_{τ_u}, respectively, of the total variance of the model, which was composed by both the variance of the random parameter and the residual variance.

To better assess the capacity of the proposed markers to discriminate between low and high CAD risk groups, the analysis was repeated

Table 3
Correlation results between the proposed markers and the demographic variables, being ρ the Pearson correlation coefficient.

	$\tau_{e,u}$		$\tau_{r,u}$		Δ_{τ_u}	
	ρ	p-value	ρ	p-value	ρ	p-value
Age	0.14	0.01	−0.12	0.04	−0.16	<0.01
BMI	0.11	0.05	−0.25	<0.01	−0.23	<0.01
Gender	–	<0.01	–	<0.01	–	<0.01

but clustering together the two low-risk groups into a new ALL-LR group. Results are shown in Fig. 9, where it can be confirmed that τ_e, τ_r and Δ_{τ} are able to distinguish between low and high CAD risk patients.

The same analysis was performed using the $d^{i,m}_{\text{QT}}(n)$ series. According to the results shown in the second half of Fig. 8 boxes, the effect of modifying the QT values at stress peak before regression parameter estimation caused the exercise lag to increase and the recovery lag to decrease. However, the tendency and significance of the lag values with CAD risk was the same: the higher the CAD risk, the larger $\overline{\tau}_{e,m}$ and the smaller $\overline{\tau}_{r,m}$.

Finally, the Spearman correlation coefficient values between the defined degree of stenosis and the proposed QT rate adaptation markers, τ_e, τ_r and Δ_{τ}, were 0.25, −0.19, and −0.24, respectively, when calculating the delays from the unmodified series, and 0.25, −0.20, and −0.21 when calculating the delays from the modified series.

4. Discussion

New biomarkers for CAD risk stratification are proposed, which estimate the time lag between the QT interval series and an estimated instantaneous memoryless QT series during the exercise and recovery phases of a stress test, being the aim to have a different, easy to estimate, QT memory value.

Computing the T-wave end in ECG signals recorded during a stress test or a high HR values is challenging. Here, we computed the QT interval series, $d_{\text{QT}}(n)$ using different variants of spatial lead transformation methodologies. Higher variance of estimated QT values is

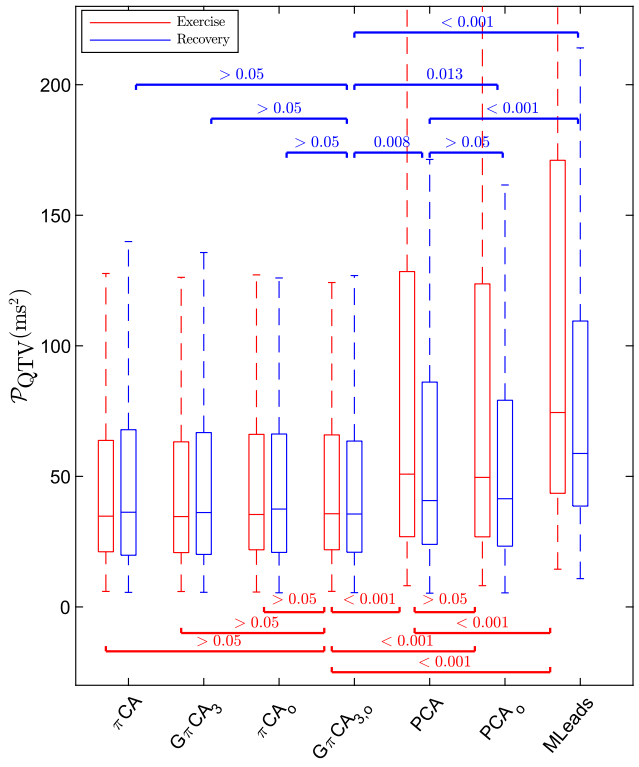

Fig. 7. QT trend fitting error quantified by $\mathcal{P}_{\mathrm{QTV}}$ power values calculated both, in exercise and in recovery, areas for delineation at TL1 in the 6 LSR techniques and for multi-lead delineation strategy, and displayed a boxplots to show the median values and extend to a maximum of 1.5 × IQR. *denote p-value < 0.001.

observed when multilead selection rules are applied to the QT values obtained on the eight independent standard leads using a wavelet-based delineator (Fig. 4a), as compared to applying the same delineator after space reduction transformations. Visual examples in Fig. 4 are in agreement with numerical quantification of the QT variability power $\mathcal{P}_{\mathrm{QTV}}$ results in Fig. 7. Computing the T-wave end in any TL1 is more stable that applying multilead delineation rules after single-lead delineation on standard leads. Concretely, better performing are obtained with πCA-based techniques than with PCA-based ones for ECG delineation during stress test. Results show that all PCA-based techniques provide similar $\mathcal{P}_{QTV}$ results and, analogously, all πCA-based techniques render similar results.

Our results are in line with previous studies that have used πCA-based techniques to emphasize beat-to-beat periodic components in Holter ECG [13,30] and found them to present superior performance than PCA or single-lead delineation strategies when high noise contamination is present.

It can be observed in Fig. 4, bottom row, that all methodologies present smooth QT traces. The large outlier contamination in Fig. 4a (top row from multi-lead delineation) clearly introduces a distortion in the median filtered trace, which could affect the lag estimation, circumstance that is clearly attenuated in the transformed lead delineation shown in Fig. 4b, and c. Other Blind Source Separation methods, as ICA, could had been considered, but the fact that πCA-based incorporates a priory available knowledge of the beat-to-beat T-wave periodicity structure, focusing on the transformation on the T-wave enhancement, lead us to restrict the analysis to πCA leaving ICA evaluation for future work developments.

To estimate the expected instantaneous memoryless, HR-dependent, QT interval series, three windows are selected, W_1, W_2 and W_3, assumed to contain stationary RR and QT series from where to estimate the α and β parameters needed in (10). Stationary series guarantee that the dominant dependency between RR and QT is mostly driven by the non-linear block, and so, well suited to estimate α and β. However, the stationarity of those segments is not really guarantee, even they are the most likely available candidates for that at the test. If the patients would have complementary ECG recordings, with better stationary conditions and with large enough ranges of RR, the α and β estimations could be redirected to those recordings.

The presented methodology implies switching the blocks of the model presented in [15] (see Fig. 2). This is motivated by the fact that the lag between $d_{RR}(n)$ and $d_{QT}(n)$ cannot be measured directly due to the different range of values of their ramps. So, the non-linear block was applied before, obtaining the instantaneous memoryless HR-dependent QT series, $d^i_{QT}(n)$. Then, this ramp-like instantaneous QT was considered as the input series of the linear first-order system, where the QT adaptation time is calculated. The non-linear relation between RR and QT, see (10), applied to the usual range of RR values, does not result in larger deviation from a ramp than those already present at RR series, see e.g. Fig. 5, and then the assumption that a ramp-like RR series implies a ramp-like QT series can be considered valid for this purpose.

Related to the identification of onset and end of the ramps for the delay computation, two considerations can be done. First, an automatic algorithm would not be necessary in cases where well annotated exercise stress onset and recovery end were available, but this is not always the case and requires extra acquisition protocol requirements. This identification can be easily dealt with the here propose algorithm. Second, the final part of the exercise ramp and the onset of the recovery ramp concur with the occurrence of a larger sympathetic activation. Consequently, the QT lag might possibly not be constant and could even decreases with the increasingly larger the sympathetic activation [17]. Therefore, we decided to limit the stress ramp to the area where the lag can be considered to remain approximately constant. The way to define these points was parameterized using the parameter γ, which can be considered a design parameter. In this work, its value was selected according to a criterion based on CAD predictive capacity.

We want to emphasize that Pearson correlation coefficient reflects modest linear relationships between the demographic variables and the proposed markers, even if p-values indicate statistical significance. This is in agreement with our results because the sign of the small correlation still indicates that patients with an elevated risk of suffering CAD are older, have a larger BMI, and $\tau_{e,u}$ is higher while both $\tau_{r,u}$ and Δ_{τ_u} are lower. In the case of gender variable, the p-values show that the marker means are different for each gender. Moreover, a linear mixed model was calculated for each proposed marker to study if the combination of the demographic variables could explain the separation of the four CAD risk groups when using the QT lag markers. The low between-group variance (3.7%, 8.2% and 9.2%) for $\tau_{e,u}$, $\tau_{r,u}$ and Δ_{τ_u} biomarkers, respectively, indicates that large delay differences are not observed between groups. Moreover, the residual variance is very high, so the proposed biomarkers cannot be explained by the demographic variables. To be sure that the last conclusion is not contaminated by the similar values between both ECG-LR and COR-LR groups, we fitted the same linear mixed model arranged in the same cluster both low-risk groups (ALL-LR). Therefore, only three risk-group can be distinguished: All-LR, COR-MR and COR-HR. We find that the new variance of the random parameter explains 4.8%, 9.3% and 10.3% for $\tau_{e,u}$, $\tau_{r,u}$ and Δ_{τ_u} biomarkers, respectively. We observe that the values have increased a little, but they are still low. Therefore, we can conclude that the combination of the three demographic parameters does not provide a linear model that represent the information of any marker. In the case that the results for the QT lag variable would be largely influenced by the confounding variables, we will expect a clearly different between the intercept of the different groups and a well-linear fitting. That means that the variance of the random parameter will be high while the residual one will be low.

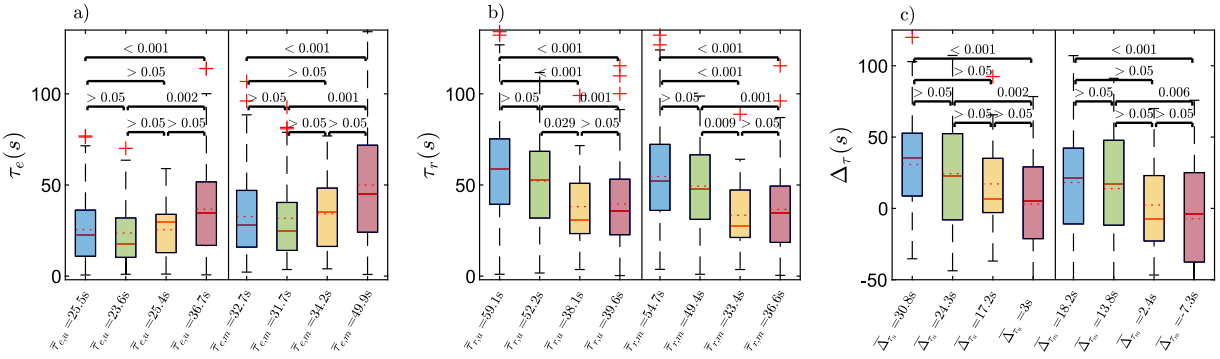

Fig. 8. Box plots of the lags between unmodified estimated $d_{QT}^{i,u}(n)$ (or modified estimated $d_{QT}^{i,m}(n)$) and real $d_{QT}(n)$ time series in (a) exercise, τ_e, and in (b) recovery, τ_r. (c) Δ_τ is the difference between recovery and exercise lags. The dotted and continuous lines inside the boxplot correspond to the mean and median values, respectively. Blue box: ECG-LR, green box: COR-LR, yellow box: COR-MR and red box: COR-HR.

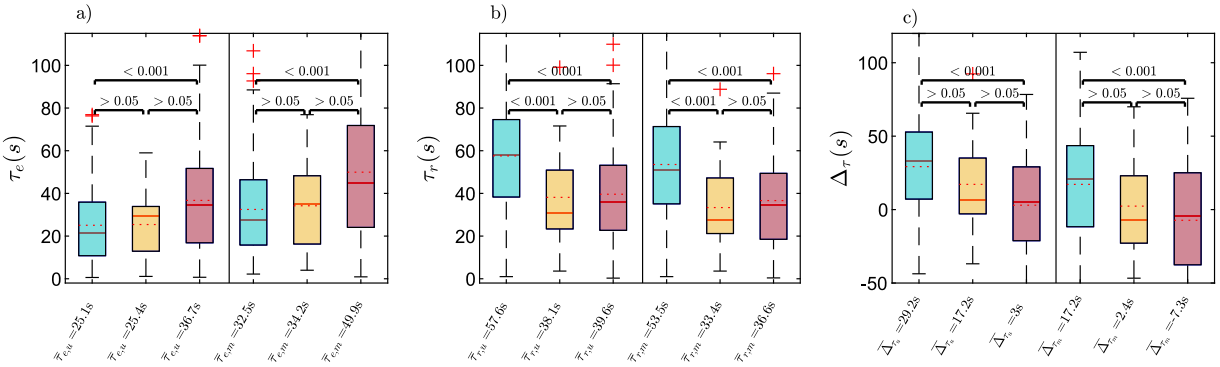

Fig. 9. After creating a new group that includes both LR groups, box plots of the lag between unmodified estimated $d_{QT}^{i,u}(n)$ (or modified estimated $d_{QT}^{i,m}(n)$) and real $d_{QT}(n)$ time series in (a) exercise, τ_e, and in (b) recovery, τ_r. (c) Δ_τ is the difference between recovery and exercise lags. The broken lines correspond to the mean values. Green box: ALL-LR, yellow box: COR-MR and red box: COR-HR.

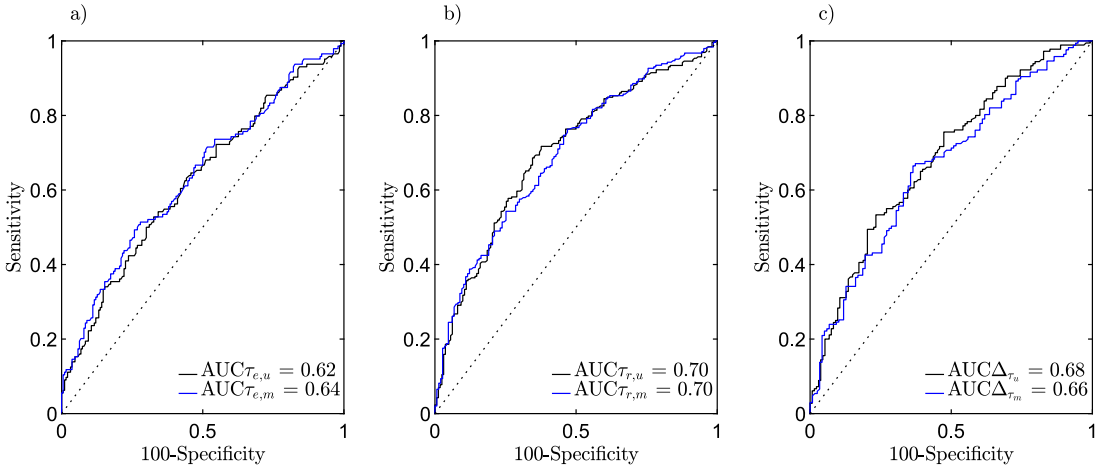

Fig. 10. (a) (b) (c): ROC curves for τ_e, τ_r and $\Delta\tau$, respectively, using as classification information the QT time lag calculated for both minor-risk groups (ECG-LR and COR-LR), and those calculated for both higher-risk groups (COR-MR and COR-HR). The analyses were done for both unmodified (black) and modified (blue) series.

The correlation values between the degree of stenosis and the three proposed QT rate adaptation markers confirm that there is a direct relationship between τ_e and CAD, that is, the degree of stenosis. However, an inverse relationship is found between τ_r (or Δ_τ) and the degree of stenosis. As described in Section 3, the Spearman correlation coefficient values did not present significant differences when computed from the unmodified or the modified QT series. The QT time lag calculated for the combination of the two low-risk groups (ECG-LR and COR-LR), and those calculated for the combination of the two high-risk groups (COR-MR and COR-HR) were clustered to compute the ROC curve for τ_e, τ_r, and Δ_τ (Fig. 10a, b, and c, respectively). The ROC curves were very similar for the delays using the unmodified series (black) and the delays using the modified series (blue) and the results point to the ability of the three QT rate adaptation markers to discriminate between low and high CAD risk. The highest stratification value was attained by the marker τ_r.

According to mean lag values calculated using unmodified QT series presented in Fig. 8, the higher the risk of suffering CAD, the higher the QT adaptation lag during exercise. This is in agreement with results reported by Lauer et al. [22] where QT hysteresis increases with the

Table 4
Comparison of presents results with published studies.

Authors	Subjects	Type of HR changes	QT adaptation time
Lau et al. [18]	7 patients with complete heart block diagnosis.	Abrupt HR changes from a temporary pacing electrode.	136 s in HR acceleration, and 189 s in HR deceleration for L_{90}.
Lauer et al. [22]	260 patients referred for treadmill exercise.	QT/RR hysteresis from gradual HR changes at stress test.	QT/RR hysteresis $\geq$ 313 s for CAD patients. QT/RR hysteresis $\geq$ 375 s for any ischemia. Higher QT/RR hysteresis is predictive of the presence and severity of myocardial ischemia.
Pueyo et al. [10]	866 patients survivors of acute myocardial infarction, of which 200 patients with the highest and lowest changes in HR were selected.	Abrupt HR changes from 24 h-Holter recordings.	From 36 to 62 s for L_{50}.
Pueyo et al. [20]	33 healthy subjects.	Abrupt HR changes from controlled postural maneuvering.	35 s in HR acceleration, and 48 s in HR deceleration for L_{90}.
Axelsson et al. [19]	25 subjects with permanent pacemakers.	Abrupt HR changes controlled by a pacemaker.	Time constant for the exponential function of the low QT adaptation phase in ventricular pacing: 50 s in HR acceleration, and 62 s in HR deceleration. 110 s in HR acceleration, and 133 s in HR deceleration for L_{90} in ventricular pacing (this phase includes both the instantaneous and the low response of the QT adaptation when the HR change).
Martin-Yebra et al. [13]	171 patients with chronic heart failure with permanent atria fibrillation.	1-h windows from ambulatory ECG recordings.	For non-SCD patients: τ = 50 s and L_{90} = 111 s. For SCD patients: τ = 67 s and L_{90} = 136 s.
Proposed	448 patients referred for a bicycle-ergometer exercise stress test.	Gradual HR changes at stress test.	For low-risk CAD patients: 25 s in HR acceleration and 57 s in HR deceleration. For high-risk CAD patients: 36 s in HR acceleration and 39 s in HR deceleration.

L_{50} and L_{90} represent the time required for QT to complete 50% and 90%, respectively, of the change in response to HR changes. τ is the delay of the first-order system with an impulse response that describing the relation between QT and RR intervals.

likelihood of any degree of ischemia or severe ischemia. In addition, the mean lag values, indicated in Fig. 8, are of the same order of magnitude as those reported in [10], where the time constants estimated from selected step-like HR changes reached values ranging from 36 to 62 s, depending on the patients. These values can be found in Table II in [10], which were measured at 50% of the complete QT adaptation time for abrupt RR changes and denoted as L50. This percent is an approximation to 63%, which corresponds to the time constant in the exponential response of a first-order system when the input is a step. So, this range is compatible with the hypothesis that time lag, measured as proposed here, at the exercise and recovery ramps or in a sudden step-like HR change protocol could provide equivalent information. Note that patients in [10] were survivors of acute myocardial infarction, while the common situation in this study is that patients are at a certain risk of suffering CAD, which correspond to different cardiac substrates.

Focusing on ECG-LR group, $\overline{\tau}_{e,u} = 25.5 \pm 17.9$ s and $\overline{\tau}_{r,u} = 59.1 \pm 27.8$ s. In [20], the mean time lag of QT interval adaptation for step-like HR change was studied independently in HR acceleration and deceleration in control subjects performing postural changes. The reported values in [20] are $\overline{\tau}_e = 34.8 \pm 13.6$ s and $\overline{\tau}_r = 48.4 \pm 25.7$ s. The larger adaptation lag in response to HR decelerations than to HR accelerations is consistent with the results in the present study. The computation of the time lag using the modified method described in 2.4.2, $\overline{\tau}_{e,m} = 32.7 \pm 22.5$ s and $\overline{\tau}_{r,m} = 52.8 \pm 32.7$ s, agree better with the values of [20]. These results suggest that the modification of the QT values at stress peak in W_2, leads to better representation of the QT-to-RR dynamics and, consequently, more accurate lag estimations.

Moreover, Axelsson et al. [19] studied the adaptation time of QT interval following an abrupt HR change, but in patients with pacemakers. They concluded that the adaptation of ventricular repolarization duration was longer after HR decrease than increase. This observation was supported by our results, see Fig. 8, although the delays of COR-HR group were practically the same in exercise and recovery. A comparison of the proposed method to measure the QT adaptation time with those reported literature is summarized in Table 4.

According to both the mean and the p-values presented in Fig. 8, the three proposed markers provide with the following information. High values of $\tau_{e,u}$ could be an indicator of a high risk of suffering CAD. This distinction is also clearly observed in Fig. 6a. $\tau_{r,u}$ and Δ_{τ_u} could be indices of suffering CAD (COR-MR and COR-HR groups) or presenting a minor risk (ECG-LR and COR-LR groups), irrespective of its severity. Attending to Δ_{τ_u} and Δ_{τ_m}, mean values decrease with the likelihood of suffering CAD, even reaching negative values or near zero.

Comparing the statistical analysis of the unmodified and modified strategies (see Fig. 8) for instantaneous QT series estimation, a small decrease in the p-values is observed for $\tau_{e,m}$ and for $\tau_{r,m}$, but retaining the statistical significance for all cases. Note that other variables like HR or QT (Table 1) also significantly discriminate between CAD groups. However, the value of the time constants estimated on stress test can provide complementary information to HR and QT and have also value for arrhythmic risk prediction as shown in [10,15] in response to abrupt HR changes. Pairwise statistical comparisons were performed. Bonferroni correction was applied considering that six comparisons were performed (p-value for statistical significance being $p < 0.008$). The significance of the results remained unaltered after applying the correction, except for the case of COR-MR vs COR-LR with $\tau_{r,m}$, which resulted in borderline significance following the correction ($p = 0.009$).

Lastly, it is worth noting that the $d_{\mathrm{QT}}^{i,u}(n)$ and $d_{\mathrm{QT}}(n)$ series became nearly overlapped, with no significant lag time, when approaching the stress peak in the exercise phase, Fig. 5b. This phenomenon is in agreement with recent findings [17] showing that the time lag for ventricular repolarization adaptation to sympathetic provocation becomes progressively reduced in response to continuously increased levels of β-adrenergic stimulation, as occurs when approaching the stress peak. Electrophysiological simulations including concurrent changes in Autonomic Nervous System (ANS) and in HR series as those studied here can shed light on the basis for this observed behavior [35].

This effect observed in the neighborhood of stress peak also explains the fact that the selected optimum thresholds for patient classification $\gamma_e^* = \gamma_r^* = 0.55$ lead to estimate lags in areas well apart from stress peak.

The main contributions of the study can be summarized as: (1) ECG delineation of a transformed lead can improve the accuracy in the identification of the T-wave end in highly contaminated ECGs as in exercise stress tests; (2) the QT time lags measured in response to ramp-like HR changes are in ranges similar to those measured in response to abrupt-like HR changes, with the evaluation of the response to HR ramps being easier to induce or observe; (3) The QT lag measured from stress test is a marker of CAD severity and can be useful for CAD diagnosis.

4.1. Study limitations and future extensions

Although GπCA shows better performance in extracting the $n_{\mathrm{Te}}(k)$ points, it has been shown preferable to compute the $n_{\mathrm{QRSo}}(k)$ points from multi-lead delineation over the 8 independent standard leads. This is a consequence of using only information from ST-T complex to learn the transformation matrix, not so well adapted to the QRS complex. If needed, a different transformation matrix could be learned for the QRS complex to improve n_{QRSo} delineation.

The robustness of the algorithm for computing the inflection point, Eq. (15), could be compromised by the stress test protocol. If the ECG recording does not include a stage before starting the exercise portion, or the recovery period is not long enough, it would be difficult to calculate the $n_{e,o}$ and $n_{r,e}$ points. In such cases, the objective function should be redefined to adapt it to the patterns of the recordings under analysis. Also, to have a proper instantaneous parametric relation estimation of the QT-to-RR relationship, HR stationary period are required, advising for prolonging the pre-test and recovery recording periods.

The number of patients in COR-MR group is small compared to the other groups. A larger variability is also observed in τ_e values of COR-MR and COR-HR groups, as compared to the LR groups. The ability of the proposed markers to separate the analyzed CAD groups suggests that these markers could be used to improve the accuracy of CAD diagnosis. A high value of the QT lag during exercise together with low values of both the QT lag during recovery and of the difference between the exercise and recovery lags could serve to identify high CAD risk. Future studies could evaluate these markers, individually or in combination with other ECG-based variables, and test their significance for CAD diagnosis in larger patient populations.

Based on the follow-up information, only 7 patients from the analyzed cohort developed SCD. Due to this limited number, the performance of the proposed biomarkers to predict SCD was not considered in the study.

The use of biophysical modeling and simulation could help to assess the role of the sympathetic nervous system in QT rate adaption measured from stress tests. Also, it could eventually help to refine the methodology here described. Simulated recordings with predetermined QT lag values and varied signal-to-noise ratios could contribute to establish the limits of the methodology and to unravel the clinically significance of the information contained in the lag.

5. Conclusion

This study shows that it is possible to quantify the QT memory as the response time lag of the QT interval to a HR ramp-like input maneuver and the estimated instantaneous memoryless expected HR-dependent QT series. A HR ramp-like-shape is found exercise and recovery areas of a stress test, where QT responds with a delayed ramp-like series to the ramp-like HR changes. This can be made as an alternative to measure the QT response to a step-like HR change, which is difficult to identify in ambulatory ECG recording or to induce with a simple test. An increase in the lag at the exercise ramp, as well as a decrease in the lag at the recovery, is found to be associated with CAD risk. The difference between lags at exercise and recovery also results in a marker for CAD risk, being remarkably larger for low-risk patients either diagnosed from the ECG or from coronary angiography, and much reduced when CAD risk increases. Same conclusions for patient clustering are obtained if the estimated instantaneous memoryless QT-to-HR fit is performed by modifying QT values at stress peak, but with absolute values in greater agreement with reported hysteresis lags values. Moreover, spatial ECG lead transformation based on πCA showed to be the best alternative to delineate the ECG and obtain the QT series in stress tests, particularly when estimating the T-wave end point. In summary, the QT memory in response to HR changes can be quantified from a stress test, obtaining values in ranges comparable to those quantified from step-like HR changes and showing clinical significance to stratify CAD risk.

Declaration of competing interest

The authors declare the following financial interests/personal relationships which may be considered as potential competing interests: Cristina reports financial support was provided by University of Zaragoza.

Data availability

The authors do not have permission to share data

Acknowledgments

This work was supported by projects PID2019-104881RB-I00, PID2019-105674RB-I00, and TED2021-130459B-I00 funded by Spanish Ministry of Science and Innovation (MICINN), Spain and FEDER, by Gobierno de Aragón (Reference Group Biomedical Signal Interpretation and Computational Simulation (BSICoS) T39-23R and project LMP94_21) cofunded by FEDER 2014–2020 "*Building Europe from Aragón*" and by European Research Council (project ERC-StG 638284). The computation was performed at the High Performance computing platform of the NANBIOSIS ICTS. C. Pérez would like to thank the support from Gobierno de Aragón with a personal PhD grant, IIU/796/2019.

References

[1] C.X. Wong, A. Brown, D.H. Lau, S.S. Chugh, C.M. Albert, J.M. Kalman, P. Sanders, Epidemiology of sudden cardiac death: global and regional perspectives, Heart Lung Circ. 28 (1) (2019) 6–14.
[2] N.V. Arteyeva, Dispersion of ventricular repolarization: Temporal and spatial, World J. Cardiol. 12 (9) (2020) 437.
[3] P. Laguna, J.P. Martínez, E. Pueyo, Techniques for ventricular repolarization instability assessment from the ECG, Proc. IEEE 104 (2) (2016).
[4] A. Pathak, D. Curnier, J. Fourcade, J. Roncalli, P.K. Stein, P. Hermant, M. Bousquet, P. Massabuau, J.-M. Sénard, J.-L. Montastruc, et al., QT dynamicity: a prognostic factor for sudden cardiac death in chronic heart failure, Eur. J. Heart Fail. 7 (2) (2005) 269–275.
[5] N.P. Johnson, T.A. Holly, J.J. Goldberger, QT dynamics early after exercise as a predictor of mortality, Heart Rhythm 7 (8) (2010) 1077–1084.
[6] S. Palacios, I. Cygankiewicz, A. Bayés de Luna, E. Pueyo, J.P. Martínez, Periodic repolarization dynamics as predictor of risk for sudden cardiac death in chronic heart failure patients, Sci. Rep. 11 (1) (2021) 1–14.
[7] M.N. Niemeijer, M.E. van den Berg, M. Eijgelsheim, G. van Herpen, B.H. Stricker, J.A. Kors, P.R. Rijnbeek, Short-term QT variability markers for the prediction of ventricular arrhythmias and sudden cardiac death: a systematic review, Heart 100 (23) (2014) 1831–1836.
[8] H. Gravel, V. Jacquemet, N. Dahdah, D. Curnier, Clinical applications of QT/RR hysteresis assessment: a systematic review, Ann. Noninvasive Electrocardiol. 23 (1) (2018) e12514.
[9] P. Kligfield, K.G. Lax, P.M. Okin, QT interval-heart rate relation during exercise in normal men and women: definition by linear regression analysis, J. Am. Coll. Cardiol. 28 (6) (1996).
[10] E. Pueyo, P. Smetana, P. Caminal, A.B. De Luna, M. Malik, P. Laguna, Characterization of QT interval adaptation to RR interval changes and its use as a risk-stratifier of arrhythmic mortality in amiodarone-treated survivors of acute myocardial infarction, IEEE Trans. Biomed. Eng. 51 (9) (2004).
[11] P. Smetana, E. Pueyo, K. Hnatkova, V. Batchvarov, P. Laguna, M. Malik, Individual patterns of dynamic QT/RR relationship in survivors of acute myocardial infarction and their relationship to antiarrhythmic efficacy of amiodarone, J. Cardiovasc. Electrophysiol. 15 (10) (2004) 1147–1154.

[12] A. Grom, T.S. Faber, M. Brunner, C. Bode, M. Zehender, Delayed adaptation of ventricular repolarization after sudden changes in heart rate due to conversion of atrial fibrillation. A potential risk factor for proarrhythmia? EP Eur. 7 (2) (2005) 113–121.
[13] A. Martín-Yebra, L. Sörnmo, P. Laguna, QT interval adaptation to heart rate changes in atrial fibrillation as a predictor of sudden cardiac death, IEEE Trans. Biomed. Eng. 69 (10) (2022) 3109–3118.
[14] D.C. Trost, A method for constructing and estimating the RR-memory of the QT-interval and its inclusion in a multivariate biomarker for torsades de pointes risk, J. Biopharm. Statist. 18 (4) (2008) 773–796.
[15] E. Pueyo, Z. Husti, T. Hornyik, I. Baczkó, P. Laguna, A. Varró, B. Rodríguez, Mechanisms of ventricular rate adaptation as a predictor of arrhythmic risk, Am. J. Physiol.-Heart Circ. Physiol. 298 (5) (2010).
[16] X. Chen, N.A. Trayanova, A novel methodology for assessing the bounded-input bounded-output instability in QT interval dynamics: application to clinical ECG with ventricular tachycardia, IEEE Trans. Biomed. Eng. 59 (8) (2011) 2111–2117.
[17] D.A. Sampedro-Puente, J. Fernandez-Bes, N. Szentandrássy, P.P. Nánasi, E. Pueyo, Time course of low-frequency oscillatory behavior in human ventricular repolarization following enhanced sympathetic activity and relation to arrhythmogenesis, Front. Physiol. 10 (2019).
[18] C.P. Lau, A.R. Freedman, S. Fleming, M. Malik, A.J. Camm, D.E. Ward, Hysteresis of the ventricular paced QT interval in response to abrupt changes in pacing rate, Cardiovasc. Res. 22 (1) (1988) 67–72.
[19] K.-J. Axelsson, L. Gransberg, G. Lundahl, F. Vahedi, L. Bergfeldt, Adaptation of ventricular repolarization time following abrupt changes in heart rate: comparisons and reproducibility of repeated atrial and ventricular pacing, Am. J. Physiol.-Heart Circ. Physiol. 320 (1) (2021) H381–H392.
[20] E. Pueyo, M. Malik, P. Laguna, A dynamic model to characterize beat-to-beat adaptation of repolarization to heart rate changes, Biomed. Signal Process. Control (2008).
[21] A. Porta, E. Tobaldini, N. Montano, RT variability unrelated to heart period and respiration progressively increases during graded head-up tilt, Am. J. Physiol.-Heart Circ. Physiol. 298 (5) (2010).
[22] M.S. Lauer, C.E. Pothier, Y.B. Chernyak, R. Brunken, M. Lieber, C. Apperson-Hansen, J.M. Starobin, Exercise-induced QT/RR-interval hysteresis as a predictor of myocardial ischemia, J. Electrocardiol. 39 (3) (2006) 315–323.
[23] K. Ogata, Modern Control Engineering, in: Instrumentation and controls series, Prentice Hall, 2010.
[24] C. Pérez, E. Pueyo, J.P. Martínez, J. Viik, P. Laguna, Characterization of impaired ventricular repolarization by quantification of QT delayed response to heart rate changes in stress test, in: Computing in Cardiology, Vol. XLVII, IEEE Computer Society, 2020, http://dx.doi.org/10.22489/CinC.2020.194.
[25] D. Charisopoulou, G. Koulaouzidis, L.F. Law, A. Rydberg, M.Y. Henein, Exercise induced worsening of mechanical heterogeneity and diastolic impairment in long QT syndrome, J. Clin. Med. 10 (1) (2020) 37.
[26] D.J. Pelchovitz, J. Ng, A.B. Chicos, D.W. Bergner, J.J. Goldberger, QT-RR hysteresis is caused by differential autonomic states during exercise and recovery, Am. J. Physiol.-Heart Circ. Physiol. 302 (12) (2012).
[27] T.M. Roston, A.M. De Souza, H.V. Romans, S. Franciosi, K.R. Armstrong, S. Sanatani, Potential overdiagnosis of long QT syndrome using exercise stress and QT stand testing in children and adolescents with a low probability of disease, J. Cardiovasc. Electrophysiol. 32 (2) (2021) 500–506.
[28] M. Virtanen, M. Kähönen, T. Nieminen, P. Karjalainen, M. Tarvainen, T. Lehtimäki, R. Lehtinen, K. Nikus, T. Kööbi, M. Niemi, et al., Heart rate variability derived from exercise ECG in the detection of coronary artery disease, Physiol. Meas. 28 (10) (2007) 1189.
[29] F. Castells, P. Laguna, L. Sörnmo, A. Bollmann, J.M. Roig, Principal component analysis in ECG signal processing, EURASIP J. Adv. Signal Process. 2007 (2007) 1–21.
[30] F. Palmieri, P. Gomis, J.E. Ruiz, D. Ferreira, A. Martín-Yebra, E. Pueyo, J.P. Martínez, J. Ramírez, P. Laguna, ECG-based monitoring of blood potassium concentration: Periodic versus principal component as lead transformation for biomarker robustness, Biomed. Signal Process. Control 68 (2021) 102719.
[31] R. Bailón, J. Mateo, S. Olmos, P. Serrano, J. García, A. Del Río, I. Ferreira, P. Laguna, Coronary artery disease diagnosis based on exercise electrocardiogram indexes from repolarisation, depolarisation and heart rate variability, Med. Biol. Eng. Comput. 41 (5) (2003) 561–571.
[32] R. Sameni, C. Jutten, M.B. Shamsollahi, Multichannel electrocardiogram decomposition using periodic component analysis, IEEE Trans. Biomed. Eng. 55 (8) (2008) 1935–1940.
[33] J.P. Martínez, R. Almeida, S. Olmos, P. Laguna, A wavelet-based ECG delineator: evaluation on standard databases, IEEE Trans. Biomed. Eng. 51 (4) (2004).
[34] R. Killick, P. Fearnhead, I. Eckley, Optimal detection of changepoints with a linear computational cost, J. Am. Stat. Assoc. 107 (2012).
[35] R. Cebollada, C. Peérez, K. Mountris, J.P. Martínez, P. Laguna, E. Pueyo, Mechanisms underlying QT interval adaptation behind heart rate during stress test, in: Computing in Cardiology, Vol. in press, IEEE Computer Society, 2021.